TOTAL STRAIN VERSION OF STRAINRANGE PARTITIONING
FOR THERMOMECHANICAL FATIGUE AT LOW STRAINS

G.R. Halford and J.F. Saltsman
NASA Lewis Research Center
Cleveland, Ohio

A new method is proposed for characterizing and predicting the thermal fatigue behavior of materials. The method is based on three recent innovations in characterizing high-temperature material behavior: (a) the bithermal concept of thermal fatigue testing, (b) advanced, nonlinear, cyclic constitutive models, and (c) the total strain version of traditional Strainrange Partitioning.

INTRODUCTION

Thermal fatigue cracking continues to present a significant economic maintenance and safety problem in the hot section of aeronautical gas turbine engines. Efforts to formulate accurate and reliable life-prediction methods at reasonable costs have also been continuing as evidenced by the proliferation of thermal fatigue life-prediction approaches over the past two decades (ref. 1). The HOST project has contributed its share of approaches, including the three approaches discussed earlier in this session by representatives of two major engine manufacturers (refs. 2 to 4). A fourth approach, which has culminated very recently from ongoing developments at the Lewis Research Center over several years, is being presented formally for the first time. Our approach capitalizes on several recent innovations in the area of high-temperature material behavior. These include (1) advanced, nonlinear, cyclic constitutive equations for thermal cycling (ref. 5), (2) the concept of bithermal fatigue (refs. 6 and 7) for characterizing failure behavior of materials subjected to thermal cycling, and (3) the total strain version (refs. 8 and 9) of the method of Strainrange Partitioning (SRP). The total strain version permits the use of more tractable total strains rather than inelastic strains, which may be incalculable in practical applications.

BACKGROUND

Strainrange Partitioning (SRP) (ref. 10) was originally formulated on an inelastic strainrange versus cyclic life basis for isothermal conditions. The approach has worked well in the high-strain, low-life regime where the inelastic strains are large enough to be determined accurately by analytical and experimental methods.

To extend the method into the low-strain, long-life regime where the inelastic strains are small and difficult to determine, it was necessary to consider the total rather than just the inelastic strainrange. Formulating SRP on a total strain basis (TS-SRP) (refs. 8 and 9) required the determination of both the inelastic and the elastic strainrange versus cyclic life relations for cycles involving creep strain. The elastic strainrange versus life relations for cycles involving creep are

influenced significantly by temperature, hold time, wave shape (PP, CC, CP, and PC), and how creep is introduced into the cycle (stress hold, strain hold, slow strain rate, etc.). To make the analysis tractable, we have assumed that the elastic life lines are displaced parallel to themselves and are parallel to the elastic life line for PP cycling. This means that for a given imposed cycle type at a specific temperature, the elastic line intercept (elastic strainrange at N_f = 1 cycle) is a function only of the time of the cycle. In the first version of TS-SRP (ref. 8), the elastic line intercept was determined by the use of an empirical equation with constants determined using data obtained from failure tests. Efforts to reduce testing requirements led to the development of an updated version of TS-SRP (ref. 9). This development was based on a derived relation between failure behavior (inelastic strainrange versus cyclic life) and flow behavior (cyclic stress-strain response) and greatly reduced the time and cost of characterizing the TS-SRP behavior of an alloy. Failure behavior is characterized readily in the high-strain, low-life regime where testing times are reasonable, and the critical flow behavior is characterized in the desired low-strain, long-life regime by cycling a specimen just long enough for the stress-strain hysteresis loop to approach stability. With this approach, the elastic line intercept can be established with a minimum of long-time testing.

Traditionally, thermomechanical fatigue[1] (TMF) resistance of materials has been estimated by conducting isothermal fatigue tests at the expected maximum temperature in the TMF cycle, with effects of creep being determined by imposing hold periods at peak tensile or compressive strain. Computer-controlled testing equipment and techniques have recently been developed to the point where thermomechanical fatigue tests can be conducted routinely, so isothermal testing is no longer as justifiable. However, true TMF cycles become difficult to control, analyze, and interpret at low strainranges, and bithermal fatigue testing has been proposed (ref. 6) to avoid this difficulty.

Existing methods for predicting TMF life of components in the low-strain regime are lacking in accuracy or generality. Thus, we have actively pursued development of a TMF life-prediction method that would overcome these deficiencies. As a starting point, we have selected the SRP method because of past successes. For example, the inelastic strain version of SRP has been successfully applied to a thermomechanical fatigue problem (ref. 11) at a strain level where the inelastic strainrange could be determined accurately and for which the life relations are temperature independent. Also, the TS-SRP version has been applied successfully to isothermal problems (refs. 8 and 9) where the inelastic strainrange cannot be determined accurately. These successes suggest that the total strain version has the potential to be extended to predict the lives of TMF cycles at low strainranges.

This report examines the extension of TS-SRP into the TMF regime by the use of a hypothetical example for the pressure vessel and piping steel alloy 2-1/4Cr-1Mo. The cyclic stress-strain-time, that is, flow response, has been determined for both thermomechanical and bithermal cycles using the Robinson flow model (ref. 5). Unfortunately, adequate TMF failure data for this alloy, especially in the low strain regime, are not available so we cannot verify the TS-SRP life predictions at this time. The characterization of an alloy by TS-SRP requires the determination of both failure and flow responses.

---

[1]The term "thermomechanical fatigue" is used to indicate variable temperature fatigue in which the mechanical strain is imposed only by externally applied loads. Temperature gradients within the test volume are not permitted.

SYMBOLS

A	general constant in empirical flow equations
A'	general constant in empirical flow equations
B	intercept of elastic strainrange versus life relation
C	intercept of inelastic strainrange versus life relation
C'	intercept of equivalent inelastic line for combined creep-fatigue cycles with parallel inelastic failure lines
CC	creep strain in tension, creep strain in compression
CP	creep strain in tension, plastic strain in compression
f	frequency
F	strain fraction
K	cyclic strain-hardening coefficient
N	number of cycles to failure
PC	plastic strain in tension, creep strain in compression
PP	plastic strain in tension, plastic strain in compression
R	mean stress correction term for nonisothermal fatigue
r	correlation coefficient
t	hold time per cycle
V	fatigue mean stress correction term; isothermal and nonisothermal
y	general dependent variable
Δ	range of variable
ϵ	strain
σ	stress
τ	period of one cycle

Subscripts:

amp	amplitude
bi	bithermal

c	compression
cc	creep strain in tension, creep strain in compression
cp	creep strain in tension, plastic strain in compression
el	elastic
eff	effective
fm	failure; mean stress condition
f0	failure; zero mean stress condition
in	inelastic
ij	pp, cc, pc, cp
m	mean
max	maximum value
min	minimum value
pc	plastic strain in tension, creep strain in compression
pp	plastic strain in tension, plastic strain in compression
pre	predicted
t	tension or total strain
tm	thermomechanical
σ	stress

Superscripts:

b	time-independent power of cyclic life for elastic strainrange versus life relation
c	power of cyclic life for inelastic strainrange versus life relations
m	general power of time in empirical flow equations
n	time-independent, cyclic strain-hardening exponent
α	power on total strainrange in empirical flow equations

Cycle type (nonisothermal):

HRIP	high-rate inphase cycle producing 100-percent PP strainrange
HROP	high-rate out-of-phase cycle producing 100-percent PP strainrange

438

THIP   tensile hold inphase cycle with hold period at maximum tensile strain produc-
        ing CP and PP strainranges

CHOP   compressive hold out-of-phase cycle with hold period at minimum compressive
        strain producing PC and PP strainranges

ANALYSIS

In formulating TS-SRP for isothermal fatigue (refs. 8 and 9), we assumed that
the inelastic and elastic strainrange versus life lines for creep-fatigue cycles are
parallel to the corresponding lines for pure fatigue or PP cycles, as shown in
figure 1. This is not an arbitrary assumption since our experience with several
alloys suggests that this is reasonable behavior for isothermal conditions. Note
that the frequency modified approach of Coffin (ref. 12) also uses parallel inelas-
tic and elastic lines. We assume, in the absence of data for guidance, that this
will also be the case for nonisothermal conditions.

Based on the above assumptions, a relationship between failure behavior and
flow behavior can be established. Failure behavior is expressed by the equations
for elastic and inelastic strainrange versus cyclic life:

$$\Delta\epsilon_{el} = B(N_{f0})^b \tag{1}$$

$$\Delta\epsilon_{in} = C'(N_{f0})^c \tag{2}$$

where

$$C' = [\Sigma F_{ij}(C_{ij})^{1/c}]^c \tag{3}$$

and

$$ij = pp, \ cc, \ pc, \ or \ cp$$

Equation (3) is derived from the interaction damage rule (IDR) of reference 13
and the four generic SRP inelastic strainrange – cyclic life relations for a theoret-
ical zero mean stress condition. In the past the inelastic line intercepts for creep
cycles (C_{pc}, C_{cp}, and C_{cc}) were taken to be independent of time. But recent devel-
opments (ref. 14) indicate that they may be time dependent at elevated temperatures,
and procedures have been proposed for expressing the time dependencies analytically.
The following development of the TMF life-prediction method based on TS-SRP will not
explicitly consider the time dependency of the inelastic lines, although it could be
added if needed.

The four generic SRP relations are

$$\Delta\epsilon_{in} = C_{ij}(N_{ij})^c \tag{4}$$

The IDR is written as follows:

$$\sum \left[\frac{F_{ij}}{N_{ij}}\right] = \frac{1}{N_{f0}} \tag{5}$$

439

where $\Sigma F_{ij} = 1.0$. Using equation (4) to solve for N_{ij} and substituting into equation (5), we obtain equation (3). Flow behavior is expressed by an equation relating elastic and inelastic strainranges:

$$\Delta\epsilon_{el} = K_{ij}(\Delta\epsilon_{in})^n \qquad (6)$$

where $n = b/c$.

Based on the assumption that the inelastic and elastic failure lines for creep-fatigue cycles are parallel to the corresponding failure lines for PP cycles, it follows that the strain-hardening exponent n in equation (6) is a constant as shown in figure 2.

For isothermal conditions the strain-hardening coefficient K_{ij} is a function of temperature, hold time, how creep is introduced into the cycle (stress hold, strain hold, etc.), and the strainrate-hardening characteristics of the alloy. For nonisothermal conditions it is also a function of the maximum and minimum temperatures and the phase relation between strain and temperature.

The time-dependent behavior of the elastic strainrange-life relation for creep cycles is shown schematically in figure 3. Setting equation (1) equal to equation (6) and eliminating N_{f0} using equation (2), we obtain the following equation relating flow and failure behavior:

$$B = K_{ij}(C')^n \qquad (7)$$

In this equation the inelastic line intercepts C_{ij} and the exponent c used to determine C' are considered to be failure terms. The strain fractions F_{ij}, the strength coefficient K_{ij}, and the strain-hardening exponent n are considered to be flow terms. Thus, the elastic line intercept B can be determined for a creep cycle from a combination of flow and failure data. Note that K_{ij} and F_{ij} will, in general, depend on waveform.

We are now in a position to establish a total strainrange versus life relation and thus predict life on a total strainrange basis. Note that the SRP inelastic strainrange versus life relations and the flow relations are determined for a specified minimum and maximum temperature and phase relationship between strain and temperature. The total strainrange is

$$\Delta\epsilon_t = \Delta\epsilon_{el} + \Delta\epsilon_{in} \qquad (8)$$

From equations (1) and (2) we obtain

$$\Delta\epsilon_t = B(N_{f0})^b + C'(N_{f0})^c \qquad (9)$$

A schematic plot of equation (9) is shown in figure 1. Note that the solution of this equation gives the cyclic life N_{f0} for a theoretical zero mean stress condition. The final step in a life prediction is to adjust the computed life to account for any mean stress effects that may be present.

A method for accounting for mean stress effects on life for isothermal conditions has been proposed in reference 15;

$$(N_{fm})^b = (N_{f0})^b - V_{eff} \qquad (10)$$

where N_{fm} and N_{f0} are the lives with and without mean stress, respectively, and V_{eff} is the effective mean stress correction term. For isothermal fatigue, V_{eff} has been determined by the following equation:

$$V_{eff} = V_\sigma \exp\left[-70\left(\frac{\Delta\epsilon_{in}}{\Delta\epsilon_{el}}\right)^2\right] \tag{11}$$

where $V_\sigma = \sigma_m/\sigma_{amp}$. Note that this method of correcting for the mean stress effect on cyclic life was developed for a specific nickel-base alloy and may not apply to other alloys or even to other nickel-base alloys. The analyst must determine that the mean stress correction equation used is applicable to the alloy of interest.

For TMF an alternate definition of V_{eff} is in order since a mean stress can naturally develop because of the temperature dependency of the yield strength in tension and compression. Hence, V_{eff} in equation (10) should be determined (ref. 1) by the following:

$$V_{eff} = \frac{1 + \dfrac{R_\sigma}{R_y}}{1 - \dfrac{R_\sigma}{R_y}} \tag{12}$$

where R_σ is equal to $\sigma_{min}/\sigma_{max}$ and R_y is the absolute value of the ratio of the compressive yield strength to the tensile yield strength at their respective maximum and minimum temperatures and strain rates in the TMF cycle. To date there is no direct experimental verification of this method for accounting for mean stress effects for nonisothermal fatigue.

To predict life on a total strainrange basis, it is necessary first to determine the PP inelastic and elastic lines and the desired SRP inelastic strainrange versus life relations experimentally. Note that these relations are to be established for a theoretical zero mean stress condition. Empirical estimation methods developed for isothermal fatigue, such as the ductility-normalized SRP relations (ref. 16) are not recommended at this time as they have not been verified for application to TMF. Ideally, failure and flow behavior would be determined from TMF tests duplicating the cycles for which lives are to be predicted. However, this approach is impractical as it lacks generality of use. For example, if the cycle were to change, the entire data base would have to be regenerated at a doubling of cost and lead time. Further changes would in turn require further repetition of experiments. A more basic approach is thus required. While an isothermal approach would offer advantages in terms of costs because of the vast background of isothermal data bases, we do not, at this time, recommend doing so. This recommendation comes as a result of an indepth survey (ref. 1) comparing the TMF and isothermal fatigue resistances of many alloys. Only under special circumstances of temperature invariant deformation and cracking mechanisms could isothermal fatigue resistance be used to accurately predict TMF results.

At this stage of development of the TS-SRP approach, we recommend resorting to bithermal fatigue tests (ref. 6) to generate the experimental inelastic strainrange-life relations required by TS-SRP. Bithermal fatigue offers the simplicity of isothermal testing, yet it captures the first-order effects of inphase and out-of-phase

TMF cycling. The bithermal tests should cover a sufficient temperature range to encompass the deformation and cracking mechanisms pertinent to the TMF cycles of interest. Determination of the critical temperature ranges for testing will require a rudimentary understanding of the metallurgical factors governing the deformation and cracking mechanisms. Thermomechanical flow tests would normally be conducted to properly characterize the stress-strain response, but bithermal flow tests could be conducted at the lower strain ranges where the inelastic strains are small and it is difficult to analyze the thermomechanical hysteresis loops. The stress-strain response of the two types of cycles should be similar in this strain regime, and the bithermal cycle would be a good approximation to the thermomechanical cycle. The thermomechanical and bithermal cycles used in this report are shown in figure 4.

Techniques are described in reference 6 for determining PP life relations for inphase and out-of-phase bithermal cycles, CP inphase, and PC out-of-phase inelastic strainrange-life relations. Proposals for the determination of a CC bithermal life relation have not been discussed because of the exclusion of such a strainrange component in TMF cycles at small inelastic strainranges.

The strain-hardening coefficient K_{ij} and the strain fraction F_{ij} can be determined using an appropriate constitutive flow model for which the material constants are available. As an alternative, they could be determined by conducting flow tests for the creep-fatigue cycles of interest. Using these data, one can determine the necessary empirical correlations describing flow behavior. The latter approach is the most viable option at this time because reliable constitutive flow models in the low strain regime and the required material constants are not yet generally available. The procedures for determining the flow correlations are described in the following section.

The strainrange analysis presented above is based on the assumption that the inelastic and elastic versus life lines for creep-fatigue cycles are parallel to the corresponding lines for PP cycles. This may not always be a satisfactory assumption. (The case of nonparallel lines is addressed in ref. 17.)

ANALYSIS USING ROBINSON CONSTITUTIVE MODEL

The choice of a constitutive model for use with TS-SRP was somewhat arbitrary. We have selected the Robinson model (refs. 5 and 18) because it has been validated for TMF application (using the alloy 2-1/4Cr-1Mo steel in the post-weld, heat-treated condition). Using Robinson's model, we have obtained the simple power law correlation shown below. This same power law form was also used successfully to correlate isothermal flow data (ref. 9):

$$y = A(t)^m \tag{13}$$

where y is the dependent variable representing several different flow variables, as will be discussed shortly, and t is the hold time per cycle.

Generally, the intercept A (value of y at $t = 1$) is a function of total strainrange. The results obtained from the Robinson model for thermomechanical cycles and earlier results for isothermal cycles using the Walker model (refs. 9 and 18) show that the family of lines shown in figure 5 can be taken as parallel. Thus, the exponent on time m is assumed to be independent of total strainrange. By a process of trial and error, we determined that the intercept A can be correlated with total strainrange by another power law as shown in figure 6;

$$A = A'(\Delta\epsilon_t)^{\alpha} \tag{14}$$

thus

$$y = A'(\Delta\epsilon)^{\alpha}(t)^m \tag{15}$$

The dependent variable y is now a function of two independent variables, $\Delta\epsilon_t$ and t. If both sides of equation (15) are divided by $(\Delta\epsilon_t)^{\alpha}$ the family of lines shown schematically in figure 5 collapse to the single line of figure 7. The values of A', α, and m vary with the dependent variable y and the mechanical properties of the alloy. Note that TS-SRP is not dependent on the form of the equation used to correlate the flow data and that equation (15) could be of many different forms. The only requirement is that it represent the flow data in a tractable form with sufficient accuracy.

Five flow correlations based on equation (15) are used herein to determine the required flow variables: K_{ij}, F_{ij}, $\Delta\sigma$, σ_t, and σ_c. The first two are used to determine the coefficients B and C' in equation (9). The remaining three are used to determine the term R_σ in the mean stress correction using equation (12).

Note that, in principle, each of these correlations could be obtained directly from a suitable constitutive model. Although the exact form of the relations would no doubt differ somewhat from the one used here, the trends would be quite similar. The empirical correlations are used only because of their extreme simplicity and comparatively good accuracy.

For a specific alloy, these correlations depend on the maximum and minimum temperature of the cycle, the wave shape, how creep is introduced into the cycle (stress hold, strain hold, etc.), the straining rate during loading and unloading, and the phase relation between strain and temperature. Only inphase and out-of-phase continuous cycles and strain-hold cycles with zero mean strain are considered at the moment. These are shown in figure 4. When computing the stresses and strains for the postulated bithermal hysteresis loops, the temperature is changed at zero stress on the tension-going and compression-going sides of the loops. And when calculating the TMF loops, the temperature ramp rate is determined by the maximum and minimum temperatures in the cycle and the mechanical straining rate. The relation between strainrate and temperature rate for a sawtooth waveform is derived in the following manner for inphase and out-of-phase cycles. For a constant strainrate,

$$\dot\epsilon = 2f(\Delta\epsilon_t) \tag{16}$$

The period of one cycle is the reciprocal of the frequency f ($\tau = 1/f$), and the temperature range is traversed in one-half the cycle period.

Let τ' equal $\tau/2$, thus the time required to go from one strain limit to the other is

$$\tau' = \frac{\Delta\epsilon_t}{\dot\epsilon} \tag{17}$$

Let ΔT equal the temperature range of the cycle of interest (inphase or out-of-phase). The temperature ramp rate $\dot{T}$ is given by the temperature range divided by the time required to traverse the cycle. Note that $\dot{T}$ is positive if the temperature is increasing and negative if the temperature is decreasing;

443

$$\dot{T} = \frac{\Delta T(\Delta \epsilon_t)}{\dot{\epsilon}}$$ (18)

Inphase and out-of-phase thermomechanical and bithermal hysteresis loop results were obtained from the Robinson model for the following conditions:

Total strainrange values:

    Continuous cycling: 0.002 to 0.010 in increments of 0.001
    Strain-hold cycling: 0.002, 0.003, 0.004, 0.006, 0.008, 0.010
    Hold time, sec: 60, 300, 600, 1800, 3600
    Minimum temperature, °C: 250
    Maximum temperature, °C: 600
    Strainrate, in./in./min: 0.04

A review of the results of these computations for the cycles considered herein reveals the following differences in the stress-strain response of the thermomechanical and bithermal cycles for a given total strainrange and hold time.

Inphase cycles	Out-of-phase cycles
$|\sigma_{t,tm}| > |\sigma_{t,bi}|$	$|\sigma_{t,tm}| < |\sigma_{t,bi}|$
$|\sigma_{c,tm}| < |\sigma_{c,bi}|$	$|\sigma_{c,tm}| > |\sigma_{c,bi}|$
$|\Delta\sigma_{tm}| < |\Delta\sigma_{bi}|$	$|\Delta\sigma_{tm}| < |\Delta\sigma_{bi}|$
$|\Delta\epsilon_{el,tm}| < |\Delta\epsilon_{el,bi}|$	$|\Delta\epsilon_{el,tm}| < |\Delta\epsilon_{el,bi}|$

The above results are as expected. For example, in an inphase bithermal cycle, the stress is acting at the maximum temperature for the entire duration of the tensile half, but in a thermomechanical cycle the stress is acting at the maximum temperature only briefly at the maximum strain limit. Thus σ_t will be greater in a thermomechanical cycle than in a bithermal cycle because of the greater thermal recovery in the bithermal cycle. A similarly based argument also applies to σ_c.

We are now able to determine the flow correlations listed above using equation (15), but first the strain-hardening exponent n in equation (6) must be determined using time-independent PP flow data. The strainrate of 0.04/min may not be fast enough to obtain time-independent (PP) deformation during loading and unloading but was the fastest rate used when the material constants for the model were determined. We have assumed that this rate produces no time-dependent inelastic strains. Note also that it is highly unlikely that the high-temperature ramp rate T implied by equation (18) could be achieved during the cooling leg of a thermomechanical cycle. Nevertheless, the following results were obtained:

$$\Delta\epsilon_{el} = 0.0045(\Delta\epsilon_{in})^{0.107}$$ (19)

for thermomechanical cycles and

$$\Delta\epsilon_{el} = 0.0044(\Delta\epsilon_{in})^{0.105}$$ (20)

for bithermal cycles. The relations for inphase and out-of-phase PP cycles are identical.

The differences between the thermomechanical and bithermal results are virtually nill under the current circumstances. These correlations are shown in figure 8 wherein the symbols represent values calculated using the Robinson model and the line represents the empirical correlation. Correlation coefficients of 0.990 and 0.995 for the thermomechanical and bithermal cycles, respectively, indicate an exceptionally good representation of the Robinson model. In the following, we present only results for TMF cycling.

Correlation Between Cyclic Strain-Hardening Coefficient and Hold Time

Equation (15) expressed for K_{ij} is as follows:

$$K_{ij} = A'(\Delta\epsilon_t)^{\alpha}(t)^m \tag{21}$$

The strain-hardening coefficient K_{ij} for each loading condition considered using the Robinson model (hold time, total strainrange, phase relation, etc.) is calculated using equation (6) and the proper value of the strain-hardening exponent from equations (19) and (20). Previously (ref. 9), K_{ij} was taken to be independent of total strainrange, but additional analysis indicates that it is a weak function of total strainrange. A multiple regression analysis of the appropriate values gives the following correlations for out-of-phase and inphase TMF cycling with $n = 0.107$:

$$\frac{K_{pc}}{(\Delta\epsilon_t)^{0.020}} = 4.689\times10^{-3}(t)^{-0.0167} \tag{22}$$

for out-of-phase cycling and

$$\frac{K_{cp}}{(\Delta\epsilon_t)^{0.037}} = 5.052\times10^{-3}(t)^{-0.0158} \tag{23}$$

for inphase cycling. These equations are represented in figure 9, and their excellent ability to correlate the calculated results is shown in figure 10.

Correlation Between Strain Fraction and Hold Time

Equation (15) expressed for F_{ij} is as follows:

$$F_{ij} = A'(\Delta\epsilon_t)^{\alpha}(t)^m \qquad F_{ij} \leq 1.0 \tag{24}$$

Analysis of the strain fraction – hold time data showed that equation (24) is not applicable over the entire range of the data. However, good correlations were obtained by dividing the data into two regimes as indicated below.

For $0.002 \leq \Delta\epsilon_t \leq 0.004$,

$$\frac{F_{pc}}{(\Delta\epsilon_t)^{-2.073}} = 1.416\times10^{-6}(t)^{0.0506} \tag{25}$$

for out-of-phase cycles and

$$\frac{F_{cp}}{(\Delta\epsilon_t)^{-2.110}} = 1.204\times10^{-6}(t)^{0.0448} \tag{26}$$

for inphase cycles. These equations are expressed in figure 11, and their ability to correlate the calculated results is represented by correlation coefficients of 0.993 and 0.994, respectively.

For $0.004 \leq \Delta\epsilon_t \leq 0.010$,

$$\frac{F_{pc}}{(\Delta\epsilon_t)^{-1.367}} = 6.062\times10^{-5}(t)^{0.0744} \tag{27}$$

for out-of-phase cycles and

$$\frac{F_{cp}}{(\Delta\epsilon_t)^{-1.364}} = 6.166\times10^{-5}(t)^{0.0733} \tag{28}$$

for inphase cycles. These equations are expressed in figure 12, and the correlation coefficients are 0.999 and 0.997, respectively. The constants for the correlations for K_{ij} and F_{ij} for TMF cycling (eqs. (21) to (28)) are summarized in table I.

Correlations Between Stress and Hold Time

Our experience suggests that better correlations for σ_t and σ_c are usually obtained when σ_t is used for cycles where creep occurs in the tensile half of the hysteresis loop (CP cycle) and when σ_c is used where creep occurs on the compressive side of the loop (PC cycle). The results obtained here show that stress is a very weak function of hold time and could be omitted with little loss of accuracy. But this may not be true generally, and we have chosen to include it for illustrative purposes. The resulting stress correlations are summarized in table IV.

LIFE PREDICTION OF TMF

In this section we outline the steps required to predict the life of a TMF cycle. For purposes of illustration, an inphase tensile strain-hold cycle (THIP) is selected. The mechanical strainrate and temperature limits are given in the previous section.

TMF cycles invariably contain both time-dependent and time-independent components of inelastic strain. Thus a THIP cycle will contain both PP and CP strain components, and the appropriate generic SRP inelastic strainrange versus life relations, equation (4), are required. Both relations must be for inphase cycling. Unfortunately, the numerical values of the material constants C_{ij} and c are not available at present. As discussed earlier, bithermal testing is recommended for determination of these material constants. For now, we proceed as if C_{ij} and c values are known;

$$\Delta\epsilon_{in} = C_{pp}(N_{pp})^c \qquad (29)$$

$$\Delta\epsilon_{in} = C_{cp}(N_{cp})^c \qquad (30)$$

The intercept C' of the equivalent inelastic line in equation (9) can now be determined. From equation (3),

$$C' = \left[F_{pp}(C_{pp})^{1/c} + F_{cp}(C_{cp})^{1/c}\right]^c \qquad (31)$$

Since $F_{pp} = 1.0 - F_{cp}$, equation (3) can be rewritten as follows:

$$C' = \left[(C_{pp})^{1/c} - F_{cp}\left[(C_{pp})^{1/c} - (C_{cp})^{1/c}\right]\right]^c \qquad (32)$$

The strain fraction F_{cp} is determined using the appropriate correlation given in the previous section.

If F_{cp} is very small ($\simeq 0$), $C' \simeq C_{pp}$; and if F_{cp} approaches unity, $C' \simeq C_{cp}$. The equivalent elastic line intercept B in equation (9) can now be determined using equation (7). The value of K_{cp} is determined using the correlation given in the previous section, and the value of C' is determined using equation (31);

$$B = K_{cp}(C')^n \qquad (33)$$

The ingredients required to make a life prediction are now available. With a knowledge of $\Delta\epsilon_t$ and the proper constants for equation (9), we can now solve for N_{f0}. The value of N_{f0} can be determined by trial-and-error or by direct use of the inversion method given in reference 19. Note that N_{f0} is the cyclic life for a theoretical zero mean stress condition (ref. 15).

The final step in a life prediction is to account for the effects of mean stress on cyclic life. Rewriting equation (10) yields

$$N_{fm} = \left[(N_{f0})^b - V_{eff}\right]^{1/b} \qquad (34)$$

The value of V_{eff} can be determined using equation (12) or some other method. If equation (12) is used, the values of σ_{min} and σ_{max} are obtained using the appropriate stress versus hold time correlations given by the constants in table II.

CONCLUDING REMARKS

The total strainrange version of Strainrange Partitioning (TS-SRP) was developed originally for isothermal fatigue. This development makes it easier to characterize an alloy and predict cyclic life in the low-strain regime without having to conduct failure tests in this regime. This development is based on a derived relation between failure behavior and the cyclic stress-strain or flow response of an alloy. Failure testing is done only in the high-strain regime where test times and costs are more reasonable, and flow testing is done in both the high- and low-strain regime. The flow tests need be run only until the stress-strain hysteresis loop approaches cyclic stability. Failure tests should also be done to determine the

effects of mean stress on cyclic life. If mean stress effects are not accounted for, inaccurate life predictions will result from using this or any other life-prediction method in the low-strain, long-life regime.

A method for extending TS-SRP to characterize an alloy and predict the lives of thermomechanical cycles in the low-strain regime is presented. This method is based on nonisothermal rather than isothermal data. Bithermal fatigue testing is recommended at this time to generate the nonisothermal data required to determine the inelastic strainrange-life relations required by TS-SRP. Bithermal fatigue testing offers the simplicity of isothermal testing but captures the first-order effects of inphase and out-of-phase TMF cycling. Thermomechanical flow tests would normally be conducted to properly characterize the stress-strain response, but bithermal flow tests could be conducted at the lower strainranges where the inelastic strains are small, and it is difficult to analyze the thermomechanical hysteresis loops.

The data from flow testing are used to determine flow response of an alloy. This response is approximated using a simple power law with two independent variables with constants determined by a multiple repression analysis. These same power law relations were used in the isothermal version of TS-SRP. It is not a requirement that this particular power law be used, since any relation could be used provided it accurately represents the data. Currently, there are no TMF data to validate the proposed life-prediction method.

REFERENCES

1. Halford, G.R.: Low-Cycle Thermal Fatigue. Thermal Stresses II, R.B. Hetnarski, ed., Elsevier, 1987, pp. 329-428.

2. Nelson, R.; and Schoendorf, J.: Cyclic Damage Accumulation Model for High Temperature Fatigue of Isotropic Hot Section Alloys. Turbine Engine Hot Section Technology 1987, NASA CP-2493, 1987, pp. 423-434.

3. Meyer, T.; Nissley, D.; and Swanson, G.: High Temperature Constitutive and Crack Initiation Modeling of Single Crystal Super alloys. Turbine Engine Hot Section Technology 1987, NASA CP-2493, 1987, pp. 401-412.

4. Kim, K.S., et al.: Elevated Temperature Crack Growth. Turbine Engine Hot Section Technology 1987, NASA CP-2493, 1987, pp. 413-422.

5. Robinson, D.N.; and Swinderman, R.W.: Unified Creep-Plasticity Constitutive Equations for 2-1/4 Cr-1Mo Steel at Elevated Temperature. ORNL/TM-8444, 1982.

6. Halford, G.R., et al.: Bithermal Fatigue, a Link Between Isothermal and Thermomechanical Fatigue. Symposium on Low Cycle Fatigue - Directions for the Future, ASTM STP-942, ASTM, 1987, pp. 625-637.

7. Gayda, J., et al.: Bithermal Low-Cycle Fatigue Behavior of a NiCoCrAlY-Coated Single Crystal Superalloy. NASA TM-89831, 1987.

8. Halford, G.R.; and Saltsman, J.F.: Strainrange Partitioning - A Total Strain Range Version. ASME International Conference on Advances in Life Prediction Methods, D.A. Woodford and J.R. Whitehead, eds., ASME, 1983, pp. 17-26.

9. Saltsman, J.F.; and Halford, G.R.: An Update of the Total Strain Version of SRP. Symposium on Low Cycle Fatigue - Directions for the Future, ASTM, STP-942, ASTM, 1987.

10. Manson, S.S.; Halford, G.R.; and Hirschberg, M.H.: Creep-Fatigue Analysis by Strain-Range Partitioning. Design for Elevated Temperature Environment, S.Y. Zamrik, ed., ASME, 1971, pp. 12-28. (NASA TM X-67838.)

11. Halford, G.R.; and Manson, S.S.: Life Prediction of Thermal-Mechanical Fatigue Using Strainrange Partitioning. Thermal Fatigue of Materials and Components, ASTM STP-612, D.A. Spera and D.F. Mowbray, eds., ASTM, 1976, pp.239-254. (NASA TM X-71829.)

12. Coffin, L.F., Jr.,: The Effect of Frequency on High Temperature Low Cycle Fatigue. Proceedings of the Air Force Conference on Fatigue and Fracture of Aircraft Structures and Materials, AFFDL-TR-70-144, 1970, pp. 301-312.

13. Manson, S.S.: The Challenge to Unify Treatment of High Temperature Fatigue - A Partisan Proposal Based on Strainrange Partitioning. Fatigue at Elevated Temperatures, ASTM STP-520, A.E. Carden, A.J. McEvily, and C.H. Wells, eds., ASTM, 1973, pp. 744-775. (NASA TM X-68171.)

14. Kalluri, S.; Manson, S.S.; and Halford, G.R.: Environmental Degradation of 316 Stainless Steel in High Temperature Fatigue, Proceedings, Third International Conference on Environmental Degradation of Engineering Materials, Penn State Univ., 1987, pp. 503-519. (NASA TM-89931.)

15. Halford, G.R.; and Nachtigall, A.J.: Strainrange Partitioning Behavior of an Advanced Gas Turbine Alloy, AFE-1DA. J. Aircr., vol. 17, no. 8, Aug. 1980, pp. 598-604.

16. Halford, G.R.; Saltsman, J.F.; and Hirschberg, M.H.: Ductility-Normalized Strainrange Partitioning Life Relations for Creep-Fatigue Life Prediction. Environmental Degradation of Engineering Materials, M.R. Louthan and R.P. McNitt, eds., Virginia Polytechnic Institute and State Univ., Blacksburg, VA, 1977, pp. 599-612.

17. Saltsman, J.F.; and Halford, G.R.: Life Prediction of Thermomechanical Fatigue Using Total Strain Version of SRP - A Proposal. NASA TP-2779, 1987.

18. Chang, T.Y.; and Thompson, R.L.: A Computer Program for Predicting Nonlinear Uniaxial Material Responses Using Viscoplastic Models. NASA TM-83675, 1984.

19. Manson, S.S.; and Muralidharan, U.: A Single Expression Formula for Inverting Strain-Life and Stress-Strain Relationships. NASA CR-165347, 1981.

TABLE I. – CONSTANTS FOR K_{ij} AND F_{ij} CORRELATIONS FOR THERMOMECHANICAL STRAIN-HOLD CYCLING
FOR $y = A'(\Delta\epsilon_t)^\alpha(t)^m$
[Material, 2-1/4CR-1Mo steel; post-weld, heat-treated condition.]

| Cycle type	Total strain-range, $\Delta\epsilon_t$	Flow variable, y	Constant, A'	Power on total strain-range, α	Power of time, m	Correlation coefficient, r
PC (out-of-phase)	--------	K_{pc}	4.689×10^{-3}	0.020	-0.0167	0.857
	0.002 to 0.004	F_{pc}	1.416×10^{-6}	-2.073	.0506	.993
	0.004 to 0.010	F_{pc}	6.062×10^{-5}	-1.367	.0744	.999
CP (inphase)	--------	K_{cp}	5.052×10^{-3}	0.037	-.0158	.929
	0.002 to 0.004	F_{cp}	1.204×10^{-6}	-2.110	.0448	.994
	0.004 to 0.010	F_{cp}	6.166×10^{-5}	-1.364	.0733	.997

TABLE II. – CONSTANTS[a] FOR STRESS CORRELATIONS FOR THERMOMECHANICAL
STRAIN-HOLD CYCLING FOR $y = A'(\Delta\epsilon_t)^\alpha(t)^m$
[Material, 2-1/4Cr-1Mo steel; post-weld, heat-treated condition.]

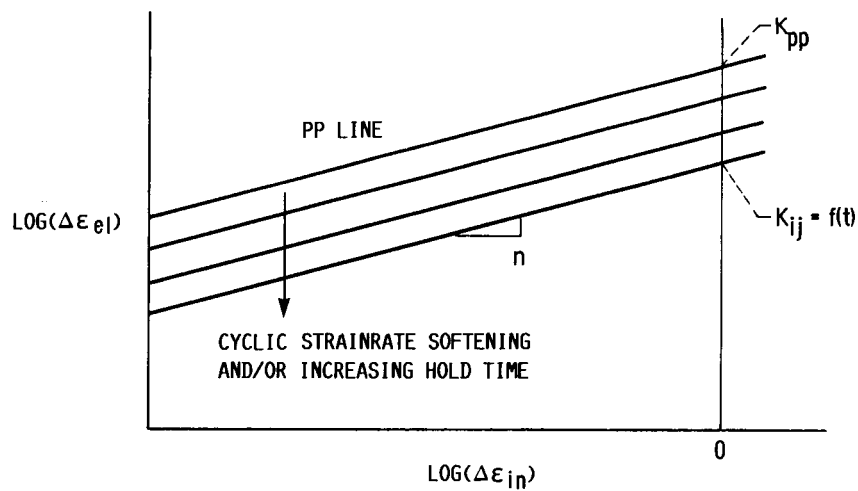| Cycle type	Flow variable, y	Constant, A'	Power on total strain-range, α	Power of time, m	Correlation coefficient, r
PC	$\Delta\sigma$	1394.7	0.230	0.0008	0.990
	σ_c	722.3	.183	.0019	.989
CP	$\Delta\sigma$	1379.8	0.227	0.0008	0.987
	σ_t	781.4	.329	.0007	.986

[a]Stresses in units of MPa (1 ksi = 6.895 MPa).

BASIS OF TOTAL STRAIN VERSION OF SRP
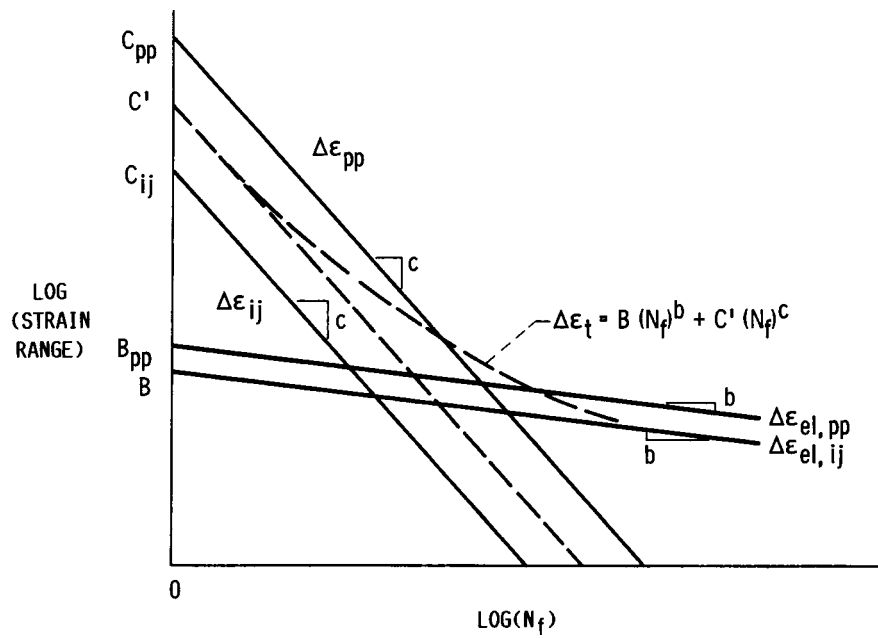
Figure 1
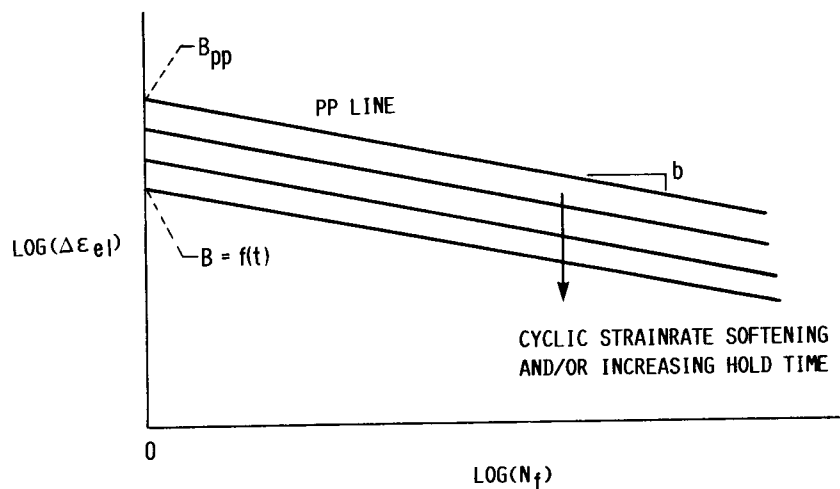
CYCLIC ELASTIC-INELASTIC STRAINRANGE RELATION DEFINING K_{ij}

Figure 2

451

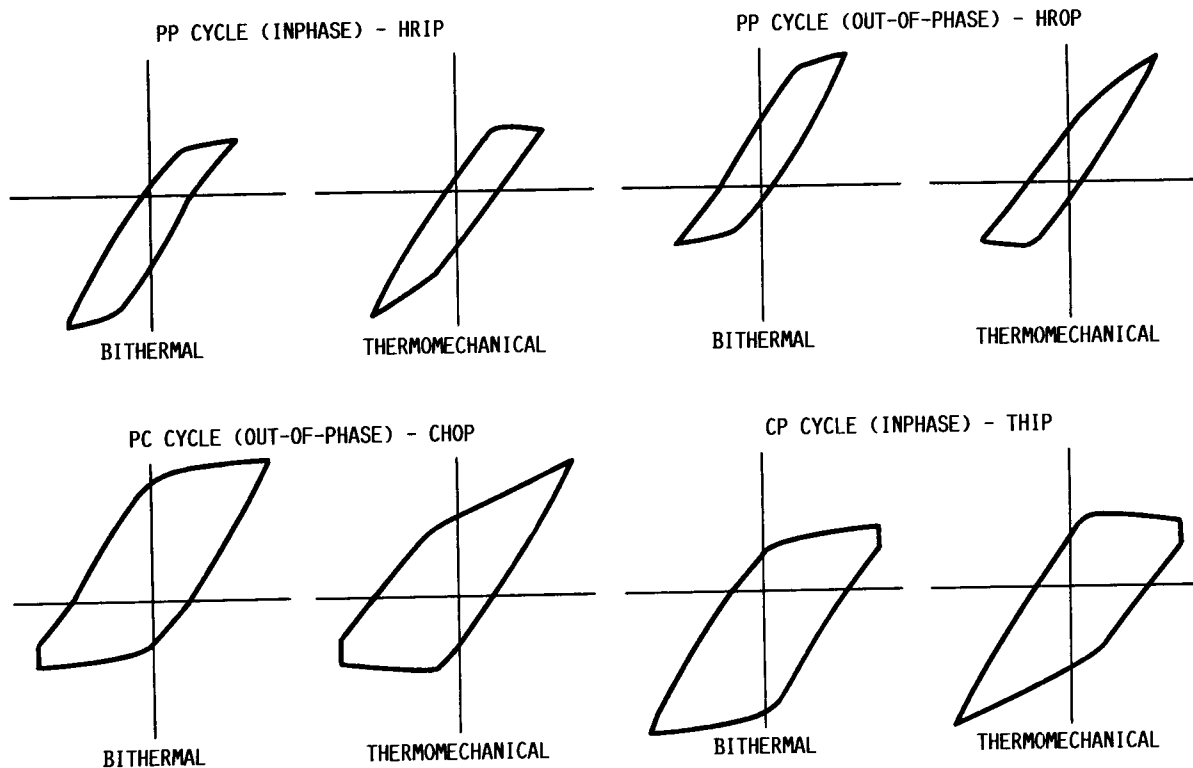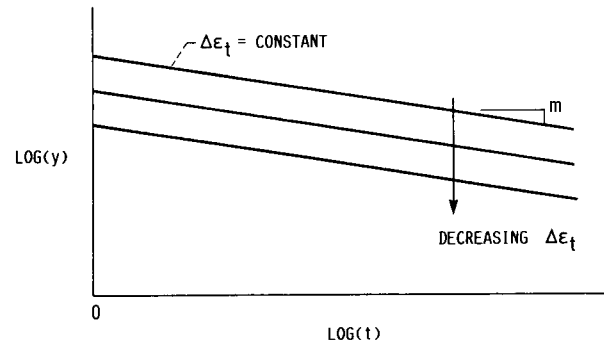# ELASTIC STRAINRANGE VERSUS LIFE RELATION DEFINING B

CD-87-29142

Figure 3

BITHERMAL AND TMF WAVE SHAPES

PP CYCLE (INPHASE) - HRIP

BITHERMAL   THERMOMECHANICAL

PP CYCLE (OUT-OF-PHASE) - HROP

BITHERMAL   THERMOMECHANICAL

PC CYCLE (OUT-OF-PHASE) - CHOP

BITHERMAL   THERMOMECHANICAL

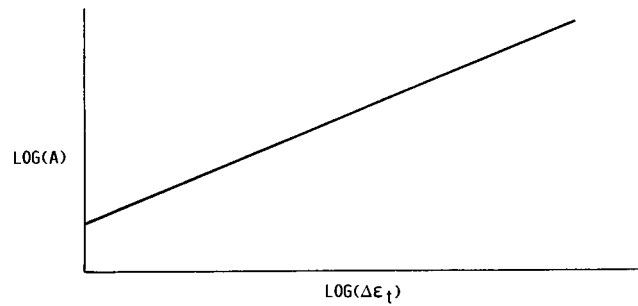CP CYCLE (INPHASE) - THIP

BITHERMAL   THERMOMECHANICAL

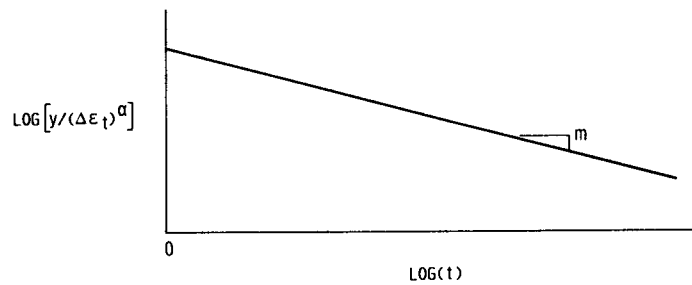CD-87-29160

Figure 4

SCHEME FOR REPRESENTING FLOW BEHAVIOR

Figure 5

BASIS FOR NORMALIZING FLOW BEHAVIOR TO TOTAL STRAINRANGE

Figure 6

NORMALIZED FLOW BEHAVIOR

Figure 7

453

POWER LAW SIMPLIFICATION OF ROBINSON'S TMF
CONSTITUTIVE MODEL FOR CYCLIC STRESS-STRAIN

2-1/4Cr-1Mo: 250 ⇌ 600 °C

THERMOMECHANICAL CYCLES (INPHASE AND OUT-OF-PHASE)

$\Delta\varepsilon_{el} = 0.0045(\Delta\varepsilon_{in})^{0.107}$
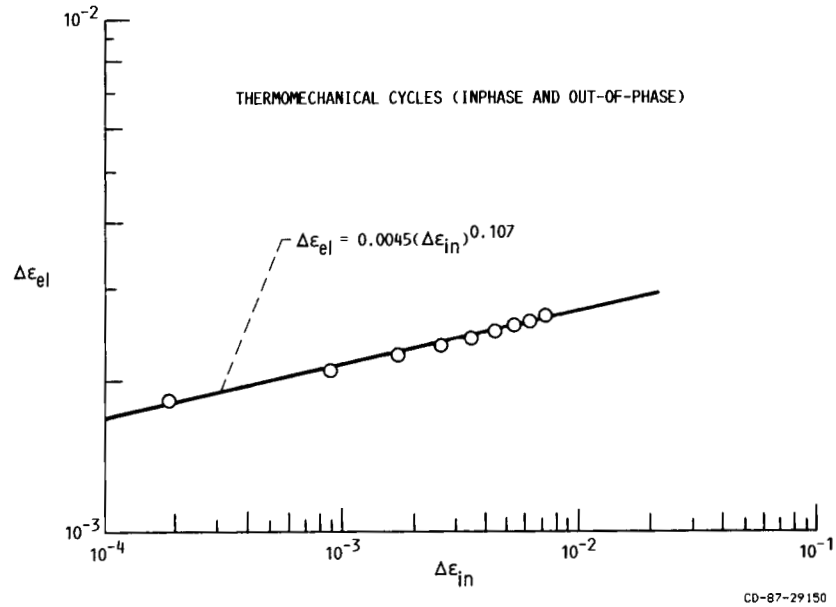
$\Delta\varepsilon_{el}$

$\Delta\varepsilon_{in}$

CD-87-29150

Figure 8(a)

POWER LAW SIMPLIFICATION OF ROBINSON'S TMF
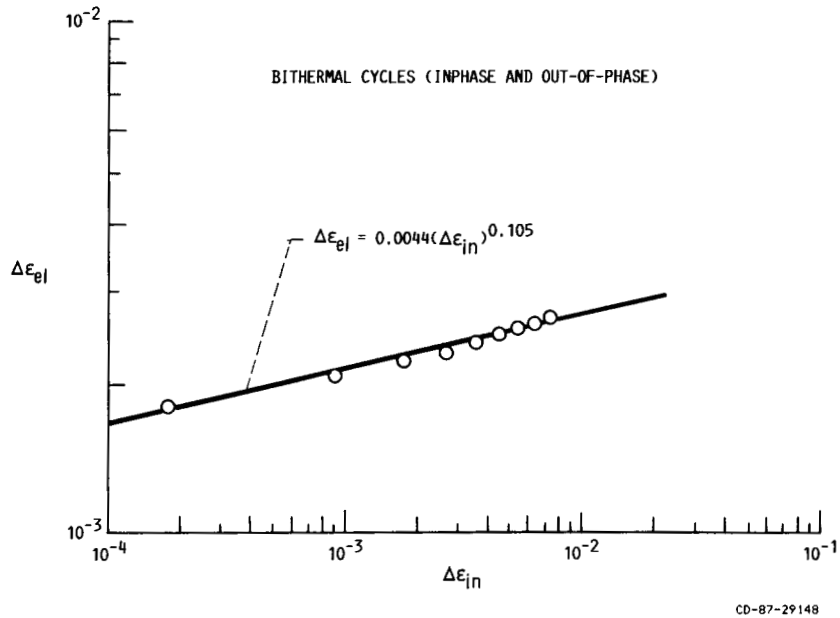# CONSTITUTIVE MODEL FOR CYCLIC STRESS-STRAIN

2-1/4Cr-1Mo: 250 ⇌ 600 °C

BITHERMAL CYCLES (INPHASE AND OUT-OF-PHASE)

$\Delta\varepsilon_{el} = 0.0044(\Delta\varepsilon_{in})^{0.105}$

$\Delta\varepsilon_{el}$

$\Delta\varepsilon_{in}$

CD-87-29148

Figure 8(b)

POWER LAW SIMPLIFICATION OF ROBINSON'S
CONSTITUTIVE MODEL FOR K_{ij}

2-1/4Cr-1Mo; 250 $\rightleftharpoons$ 600 °C

OUT-OF-PHASE TMF (PC)
n = 0.107

$$\frac{K_{pc}}{(\Delta \varepsilon_t)^{0.020}} = 4.689 \times 10^{-3} (t)^{-0.0167}$$

K_{ij}

HOLD TIME, SEC

CO-87-29151
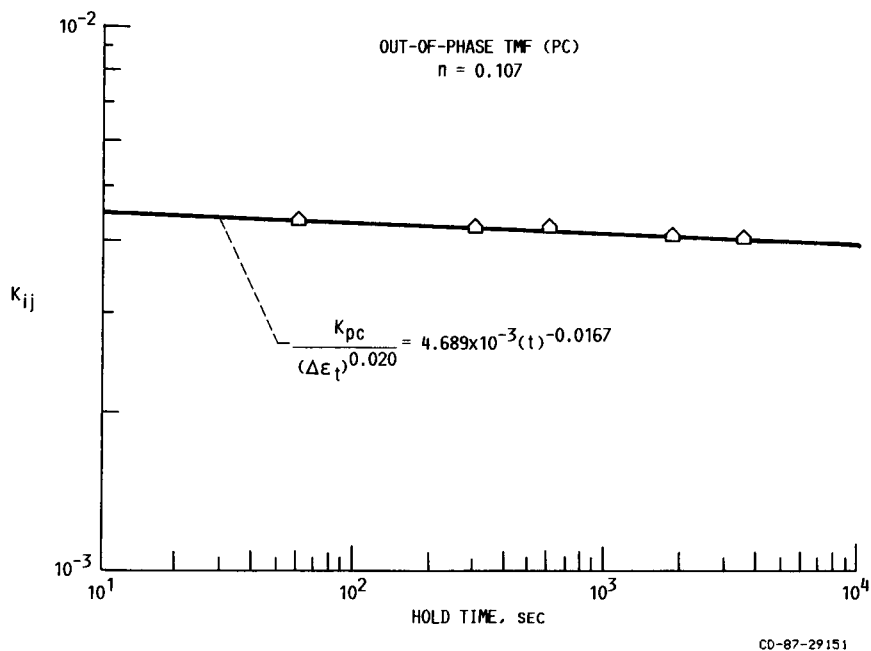
Figure 9(a)

POWER LAW SIMPLIFICATION OF ROBINSON'S TMF
CONSTITUTIVE MODEL FOR K_{ij}

2-1/4Cr-1Mo; 250 $\rightleftharpoons$ 600 °C

OUT-OF-PHASE TMF (PC)
n = 0.107

$$\frac{K_{cp}}{(\Delta \varepsilon_t)^{0.037}} = 5.052 \times 10^{-3} (t)^{-0.0158}$$

K_{ij}

HOLD TIME, SEC

CO-87-29152

Figure 9(b)

455

CORRELATION OF K_{ij} FOR TMF CYCLING TMF (PC)

2-1/4Cr-1Mo; 250 ⇋ 600 °C

$$\frac{K_{pc}}{(\Delta\varepsilon_t)^{0.020}} = 4.689 \times 10^{-3}(t)^{-0.0167}$$

OBSERVED / PREDICTED

HOLD TIME, SEC
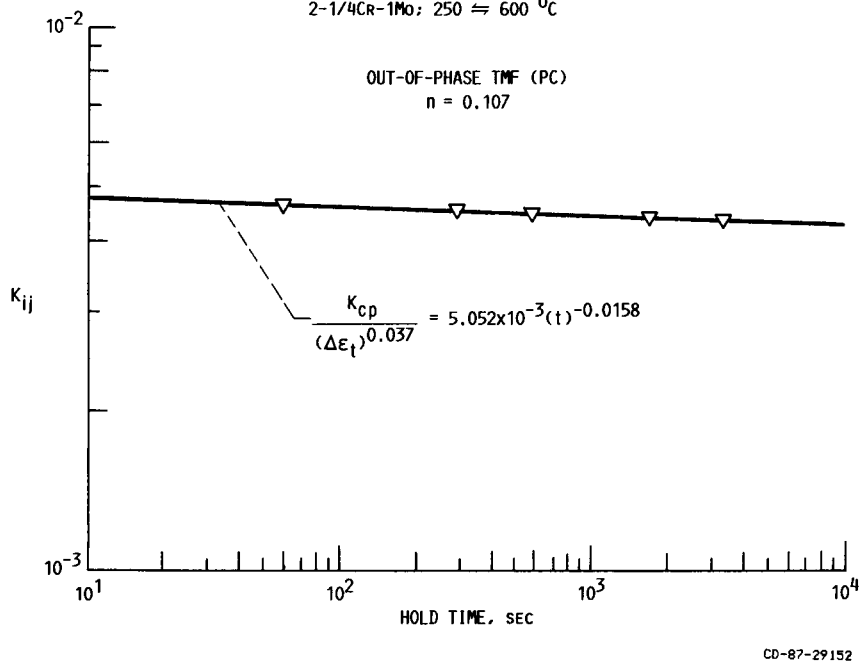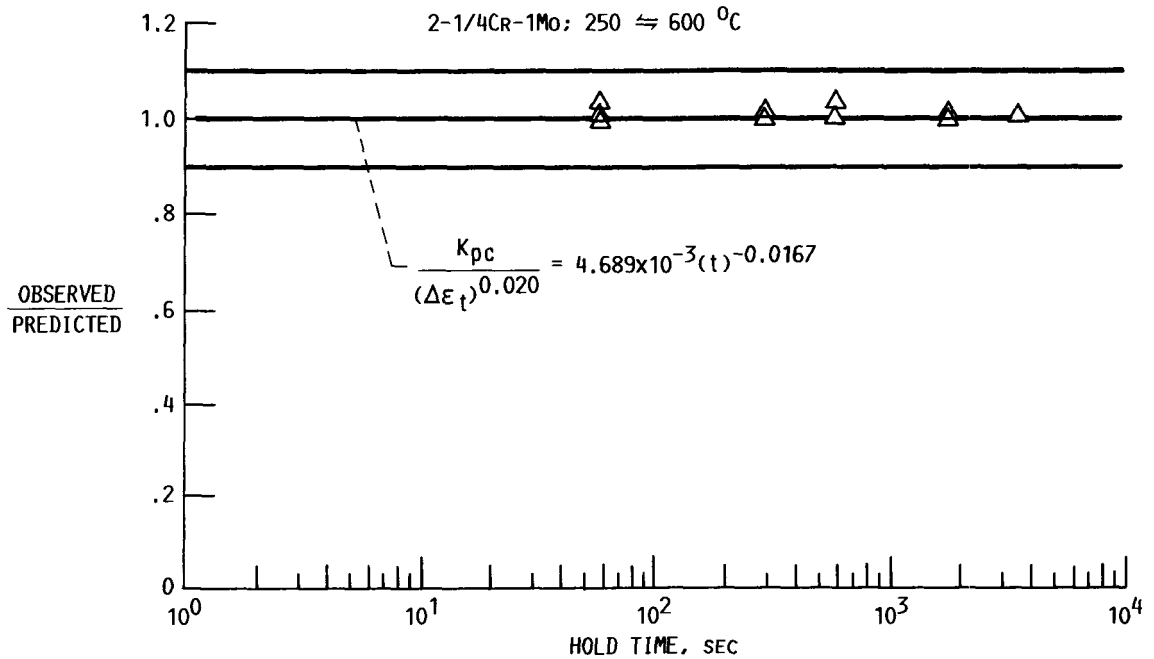
CD-87-29153

Figure 10(a)

CORRELATION OF K_{ij} FOR TMF CYCLING

2-1/4Cr-1Mo; 250 ⇋ 600 °C

TMF (CP)

$$\frac{K_{cp}}{(\Delta\varepsilon_t)^{0.037}} = 5.052 \times 10^{-3}(t)^{-0.0158}$$

OBSERVED / PREDICTED

HOLD TIME, SEC
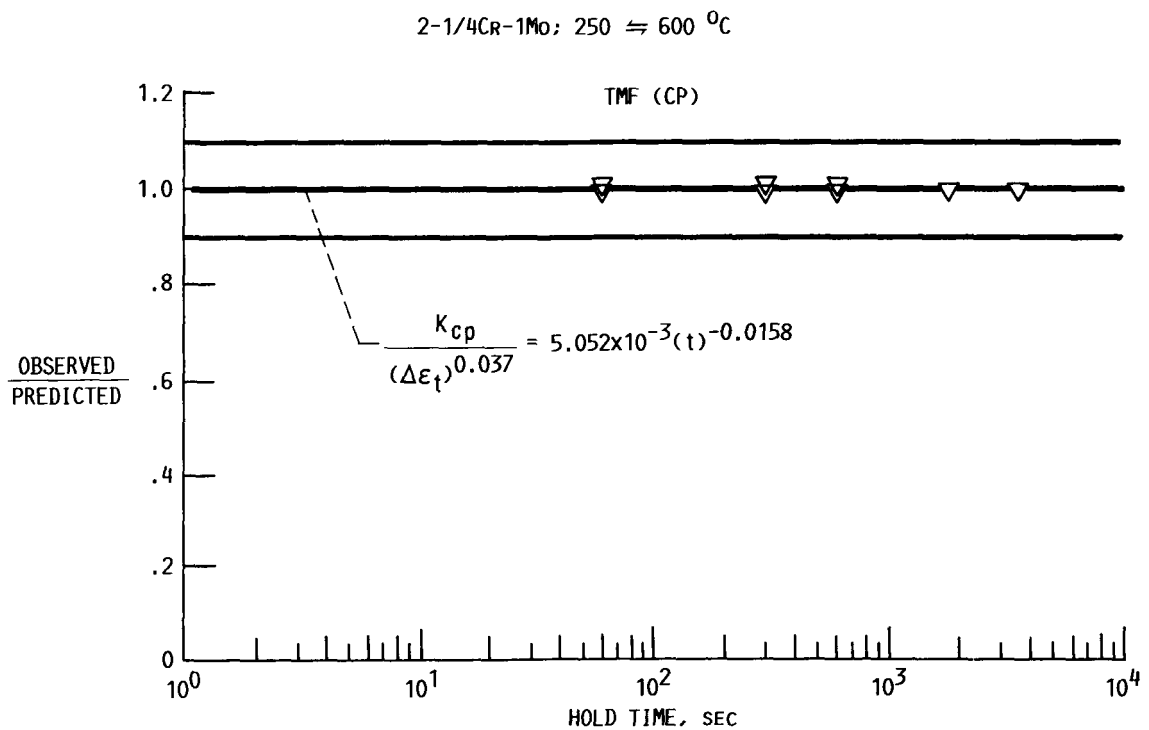
CD-87-29154

Figure 10(b)

POWER LAW SIMPLIFICATION OF ROBINSON'S TMF CONSTITUTIVE MODEL FOR F_{ij}

$2\text{-}1/4C_R\text{-}1M_O;\ 250 \leftrightharpoons 600\ {}^{\circ}C$

$0.002 \leq \Delta\varepsilon_t \leq 0.004$
TMF (PC)

$$\frac{F_{pc}}{(\Delta\varepsilon_t)^{-2.073}} = 1.416 \times 10^{-6}(t)^{0.0506}$$

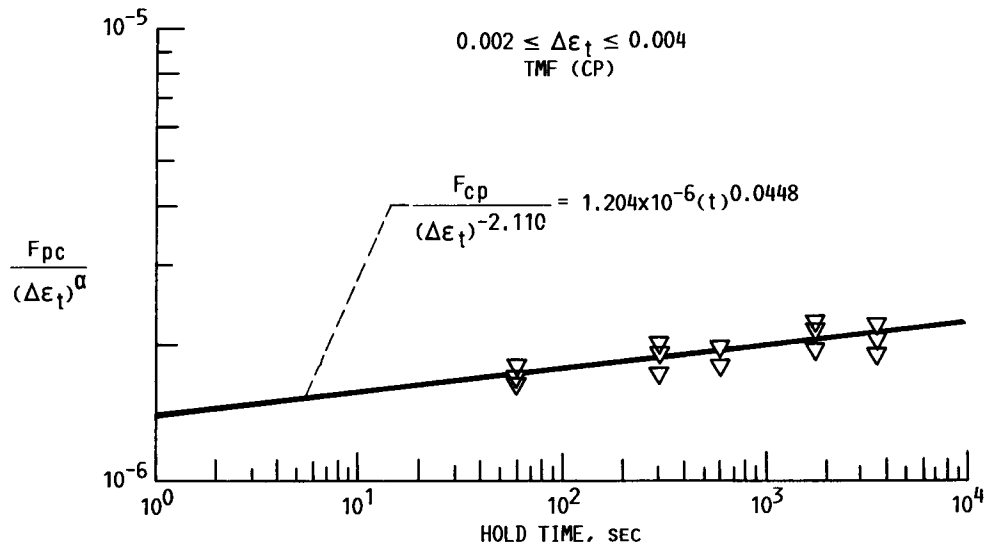y-axis: $\dfrac{F_{pc}}{(\Delta\varepsilon_t)^{\alpha}}$

x-axis: HOLD TIME, SEC
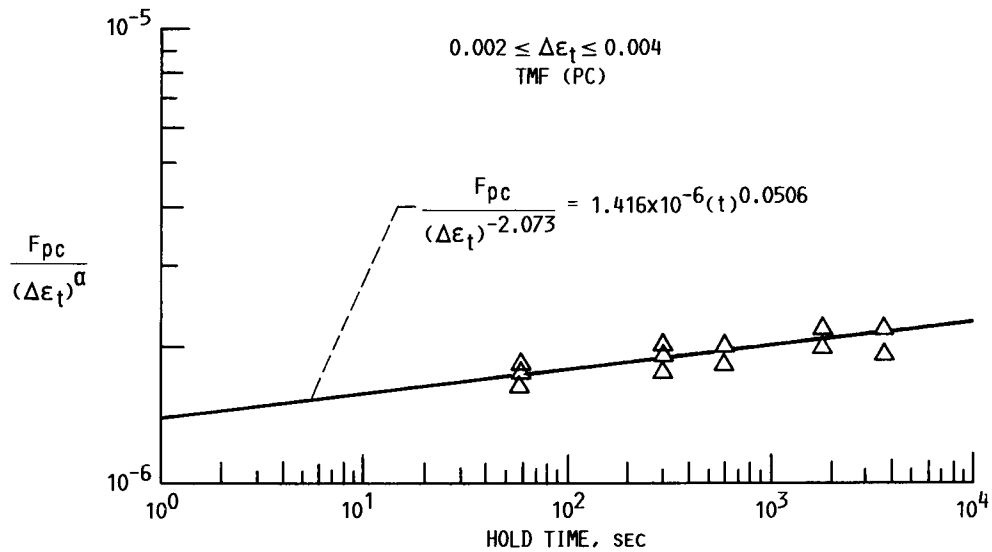
CD-87-29155

Figure 11(a)

POWER LAW SIMPLIFICATION OF ROBINSON'S TMF CONSTITUTIVE MODEL FOR F_{ij}

$2\text{-}1/4C_R\text{-}1M_O;\ 250 \leftrightharpoons 600\ {}^{\circ}C$

$0.002 \leq \Delta\varepsilon_t \leq 0.004$
TMF (CP)

$$\frac{F_{cp}}{(\Delta\varepsilon_t)^{-2.110}} = 1.204 \times 10^{-6}(t)^{0.0448}$$

y-axis: $\dfrac{F_{pc}}{(\Delta\varepsilon_t)^{\alpha}}$

x-axis: HOLD TIME, SEC

CD-87-29156

Figure 11(b)

457

POWER LAW SIMPLIFICATION OF ROBINSON'S TMF CONSTITUTIVE MODEL FOR F_{ij}

2-1/4CR-1Mo; 250 ⇌ 600 °C

$0.004 \leq \Delta\varepsilon_t \leq 0.010$
TMF (PC)

$\dfrac{F_{pc}}{(\Delta\varepsilon_t)^{-1.367}} = 6.062 \times 10^{-5} (t)^{-0.0744}$

HOLD TIME, SEC

CD-87-29157

Figure 12(a)

POWER LAW SIMPLIFICATION OF ROBINSON'S TMF CONSTITUTIVE MODEL FOR F_{ij}

2-1/4CR-1Mo; 250 ⇌ 600 °C

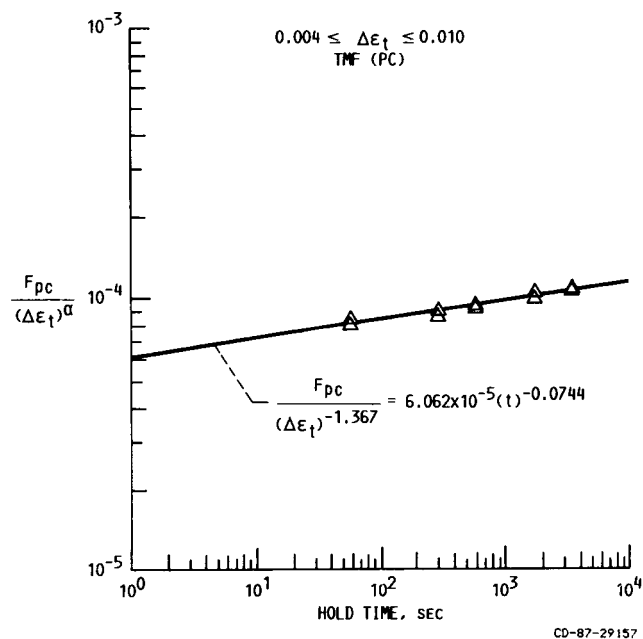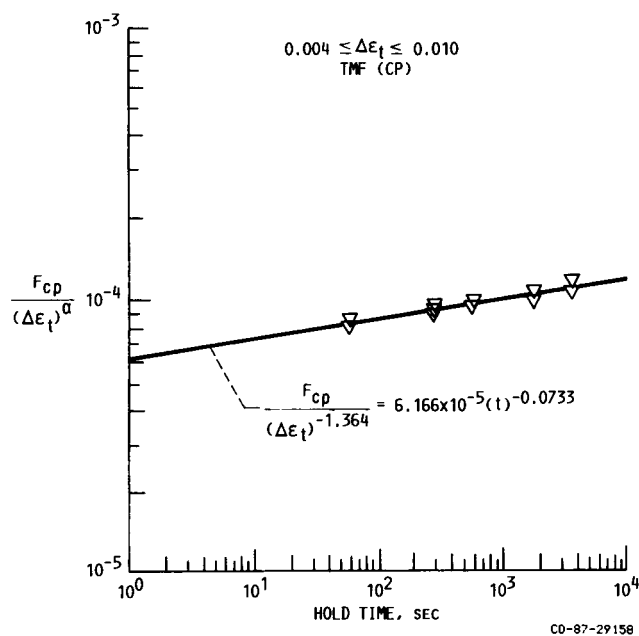$0.004 \leq \Delta\varepsilon_t \leq 0.010$
TMF (CP)

$\dfrac{F_{cp}}{(\Delta\varepsilon_t)^{-1.364}} = 6.166 \times 10^{-5} (t)^{-0.0733}$

HOLD TIME, SEC

CD-87-29158

Figure 12(b)

458